Journal of the European Ceramic Society **14** (1994) 447–453

The Brittle/Ductile Transition in Cubic Stabilised Zirconia

T. J. Marrow,[a] S. G. Roberts[b] & A. K. Pearce-Higgins[b]

[a] School of Metallurgy and Materials Science, University of Birmingham, Edgbaston, Birmingham B15 2TT, UK
[b] Department of Materials, Oxford University, Parks Road, Oxford OX1 3PH, UK

(Received 7 March 1994; accepted 17 May 1994)

Abstract

Cubic zirconia has a smooth brittle/ductile transition above 800°C at a loading rate of 1·2 × 10⁻⁴ MPa√m s⁻¹. Pre-stressing at 950°C increases the room temperature fracture toughness in a controllable manner. The toughness increase is caused by dislocation shielding of the crack tip and may be predicted using a model for dislocation generation by crack tip dislocation sources.

Kubisches Zirkoniumoxid besitzt bei einer Temperatur von über 800°C und bei Lastraten von 1·2 × 10⁻⁴ MPa√m s⁻¹ einen fließenden Übergang von sprödem zu zähem Verhalten. Durch eine vorausgehende Belastung bei 950°C kann die Raumtemperaturbruchzähigkeit in kontrollierbarer Weise erhöht werden. Die Zähigkeitszunahme wird durch die Abschirmung der Rißspitze durch Versetzungen verursacht und kann mit Hilfe eines Modelles bestimmt werden, das die Bildung von Versetzungen an der Rißspitze annimmt.

La zircone cubique présente une transition fragile/ductile au-dessus de 800°C sous une vitesse de mise en charge de 1·2 × 10⁻⁴ MPa√m s⁻¹. Une précontrainte à 950°C accroît la résistance à la rupture à température ambiante. Cette amélioration est due à un effet d'écrantage par des dislocations en front de fissure et peut être prédit à partir d'un modèle de génération de dislocations par des sources de dislocations en front de fissure.

1 Introduction

The brittle/ductile transition, i.e. the temperature and strain-rate sensitive transition from brittle fracture to general yielding of material containing a sharp pre-crack under stress, is generally determined by competition between cleavage fracture mechanisms and dislocation activity at or in the region of the crack tip. An understanding of the phenomenon is of considerable importance to fundamental fracture research. Dynamic simulations of dislocation emission, motion and the mutual interaction of the elastic stress fields of individual dislocations and crack tip have shown good agreement with the observed brittle/ductile transitions in silicon,[1–5] sapphire,[6] molybdenum[4] and germanium.[7] The temperature and form of the transition is determined by the effects of strain rate and temperature on dislocation mobility, the relative geometry of cleavage and dislocation glide planes and the distribution of dislocation sources. The general applicability of the dynamic dislocation shielding model is further tested in this paper via a comparison of the experimentally determined brittle/ductile transition in cubic stabilised zirconia with the behaviour predicted by the model.

Indentation studies of cubic zirconia stabilised with 9·4–14·6 mol% yttria (Y_2O_3)[8–11] show that cubic zirconia cleaves on {110} with a fracture toughness of around 1.1 MPa√m.[8,9] Notched test specimens gave fracture toughness values of approximately 1·5 MPa√m[9] and 2 MPa√m,[11] although neither value was corrected for the finite notch width. {001} and {111} are not good cleavage planes.[8,9]

Compression tests above 1200°C on cubic zirconia, stabilised by 9·4–18 mol% yttria (Y_2O_3–ZrO_2) and 12 mol% calcia (CaO–ZrO_2), demonstrated solid solution hardening and preferential slip on {001}⟨110⟩.[12,13] Dislocation climb and recovery were extensive and the work hardening rate was low. Preferential slip on {001} has also been indicated by hardness anisotropy in 14 mol% CaO-ZrO_2 and 14·8 mol% Y_2O_3–ZrO_2. The anisotropy decreased in magnitude with increasing tempera-

Journal of the European Ceramic Society 0955-2219/94/$7.00

ture up to 600°C.[14] High temperature slip on {111}⟨110⟩ has also been observed following indentation of 9·5 mol% Y_2O_3–ZrO_2 up to 1300°C.[10]

A smooth brittle/ductile transition has been observed in 14·6 mol% Y_2O_3–ZrO_2 using notched specimens.[15] Specimens were randomly oriented about [110] with the notch cut parallel to {110}. The strain rate was unspecified. The increase in fracture toughness above 1000°C was attributed to plastic yield of the specimen. Radial cracking along {110} nucleated by high temperature indentations in 9·4 mol% Y_2O_3–ZrO_2 showed a brittle/ductile transition with the gradual cessation of cracking between 500°C and 800°C.[10] Cleavage may be caused by Cottrell-type dislocation interactions at lower temperatures. The tendency for cracking decreased with increasing temperature as elastic stresses were relieved by plastic deformation.

This paper deals with the brittle/ductile transition of cubic zirconia (stabilised with 12·1 mol% Y_2O_3) using test specimens which contain a well-defined sharp {110} pre-crack. The results are compared with simulations from the dynamic model for the dislocation mobility controlled brittle/ductile transition.

2 Experimental Details and Results

2.1 The brittle/ductile transition

The fracture specimens were rectangular bars, measuring nominally 25mm × 1·5mm × 0·7mm, which were polished on all faces, finishing with 1 μm diamond paste. The specimens were oriented as in Fig. 1. The largest face was parallel to (001) with the long axis parallel to [110]. The specimens were pre-cracked using a 200g Knoop indentation on the (001) face. The long axis of the indenter was perpendicular to [110], producing a (110) median crack. The indented surface was polished to remove the indentation and the bulk of the indentation plastic zone (so as to relieve residual stresses from the indentation). After polishing, the pre-cracks were approximately semicircular with a mean crack depth of 25 μm. The fracture tests were conducted by four-point bending, with inner and outer spans of 12 mm and 22 mm. Fracture tests were performed in air up to 1000°C, using a high-purity alumina jig in a furnace heated by SiC elements. This was mounted on a screw-driven testing machine. Thin silicon pads, measuring approximately 0·4 mm thick, were inserted between the zirconia specimen and the loading points. The pads deformed under load and virtually eliminated failures initiated by uneven contact at the loading points for the high-temperature tests. The test cell was heated from room temperature at 3°C min^{-1} with the specimens unloaded, and was held at temperature for at least 30 min before loading. Except where noted, all high-temperature tests were conducted at a crosshead displacement rate of 1 μm min^{-1}. Some room-temperature tests were loaded at 1 mm min^{-1}.

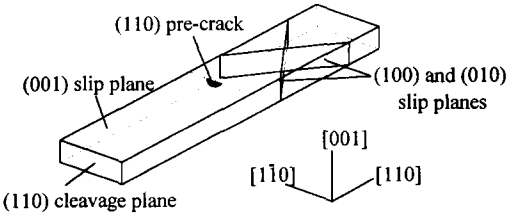

Fig. 1. The orientation of (110) cleavage plane and {001} slip planes in the cubic zirconia fracture specimens.

The crack depth and aspect ratio were determined for each specimen by post-failure optical microscopy. The stress intensity at fracture was then calculated using the standard solution for a rectangular bar containing a semi-elliptical flaw under a bending moment.[16] The variation of mode I stress intensity around the crack circumference was calculated. This was found to be less than 10% and the average value of the stress intensity at deepest point and the specimen surface was used.

The results for all specimens are shown in Fig. 2. The mean room temperature fracture toughness was 1·1 MPa$\sqrt{m}$. The fracture toughness at 1 μm min^{-1} increased smoothly between 800°C and 975°C from 1·5 MPa$\sqrt{m}$ to 2·9 MPa$\sqrt{m}$. All tests below 1000°C showed a linear load/displacement trace and fracture initiated at the pre-crack. At 1000°C the load/displacement trace showed non-linearity, due to yielding, at a surface stress of approximately 660 MPa, equivalent to a stress intensity of 4·3 MPa$\sqrt{m}$ for a crack of average size. The specimen shattered at a surface stress of over 1150 MPa. {100} slip traces were found on the (001) surface. No slip traces were observed in any other test. Increasing the crosshead displacement rate to 1 mm min^{-1} at 1000°C produced a brittle failure with a fracture toughness of 1·4 MPa$\sqrt{m}$.

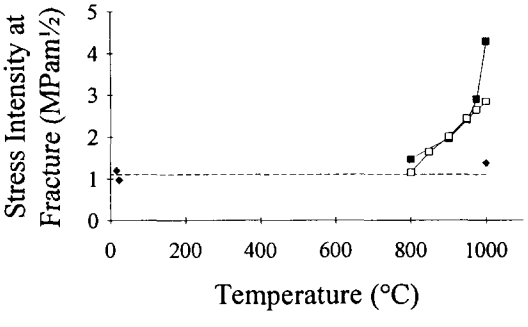

Fig. 2. The effect of temperature and loading rate on the fracture toughness of cubic zirconia, compared with the fracture toughness predicted by the dislocation shielding model. Each point corresponds to a single test. ◆, 1 mm min^{-1}; ■, 1 μm min^{-1}; □, predicted transition; – – –, 1·1 MPa $m^{1/2}$.

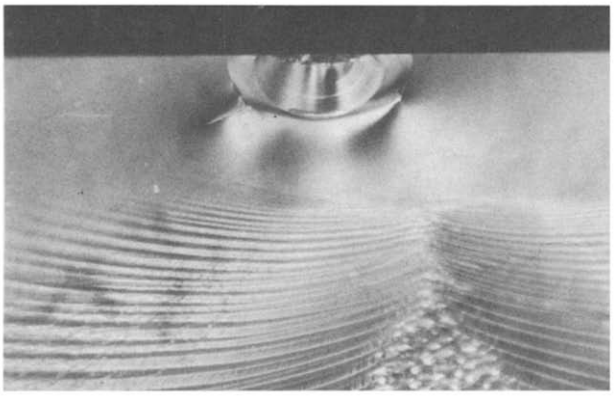

Fig. 3. Optical micrograph of the (110) fracture surface, showing semi-elliptical precrack. Tested at 1 μ min $^{-1}$ at 900°C.

2.2 Fractography and dislocation etching

Fracture surfaces were inspected using optical microscopy, and after gold-sputtering were examined by scanning electron microscopy (SEM). No significant changes in the appearance of the fracture surfaces with test temperature could be discerned (Fig. 3). The fracture surfaces were etched with molten potassium hydroxide (KOH) in a nickel crucible at 350–400°C for over 10 mins, so as to observe any dislocation activity. Unstressed samples showed etch pits on the (001) surface with an average density of approximately 10^{10} pits m^{-2}. A much higher pit density was found at the indentation site on the (001) surface of high temperature tests. The heavily etched zone measured approximately 30 μm × 10 μm.

A test at 1000°C which had failed from a loading point at an applied stress intensity of 2·3 MPa$\sqrt{m}$, loaded at 1 μm min^{-1}, was subsequently broken at the pre-crack. Etching for 40 min produced fine markings on the fracture surface, with a density of approximately 10^{12} marks m^{-2}. Optical microscopy implied these were depressions in the fracture surface (Fig. 4(a)). However, on closer examination using SEM they were found to be raised above the surface (Fig. 4(b)). Similar markings were found in smaller numbers on tests at 975°C and 950°C. No such marks were seen on the room-temperature fracture surfaces after etching. The high-temperature tests showed a tendency for localised etch attack of the crack tip not seen in specimens tested at room temperature (Fig. 4(b)).

2.3 Warm pre-stressing

Warm pre-stressing experiments were conducted at 950°C by loading pre-cracked specimens, at 1 μm min^{-1}, to stress intensity levels above the room-temperature fracture toughness. The stressed specimens were rapidly unloaded then cooled at approximately 1°C s^{-1} to room temperature. They were

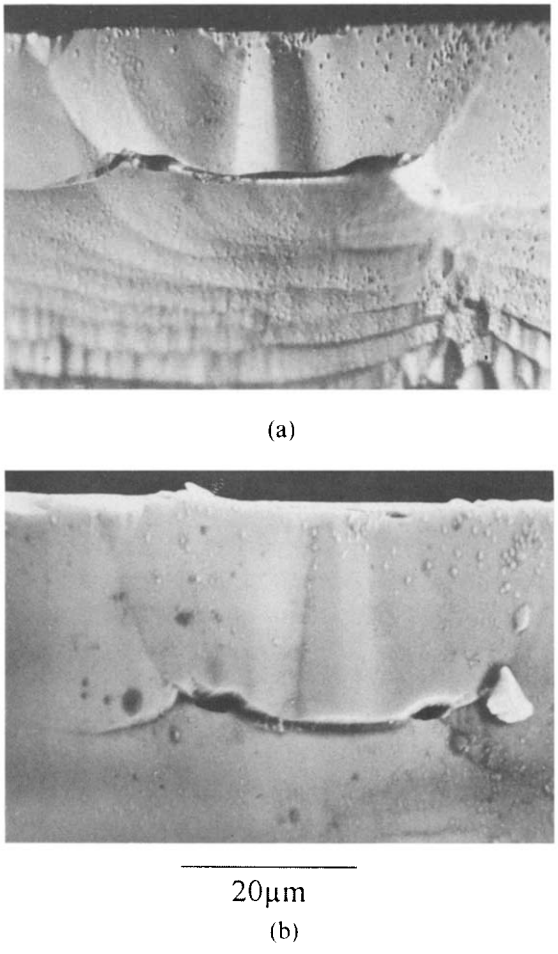

Fig. 4. Features produced by a 40 min etch in molten KOH (350°C) on the fracture surface of an interrupted slow strain rate test at 1000°C: (a) optical micrograph; (b) scanning electron micrograph.

subsequently fractured at room temperature at a loading rate of 1 mm min^{-1}. The room-temperature stress intensity at fracture was above the normal fracture toughness value (1·1 MPa$\sqrt{m}$) and increased with increasing pre-stressing stress intensity. The results are shown in Fig. 5.

2.4 Indentation testing

The room-temperature fracture toughness was determined independently using the standard indentation technique. Indentations were made using a Vickers indenter with loads between 100 g and 1000 g. The indenter diagonals were aligned parallel to ⟨110⟩ on the (001) surface. The Vickers hardness was 16·71 ± 2 GPa, and was approximately independent of load. Lateral cracking was not often observed, even at the highest loads used. Knoop indentations on (001), aligned as in the pre-cracking procedure, gave decreasing values of hardness with increasing load. Significant lateral cracking was observed above 300 g. The hardness for a 200 g load was 14·4 + 0·6 GPa. The ratio of hardness to elastic modulus (H/E) was determined from the Knoop indentation elastic relaxation,[17] giving a value of 0·037.

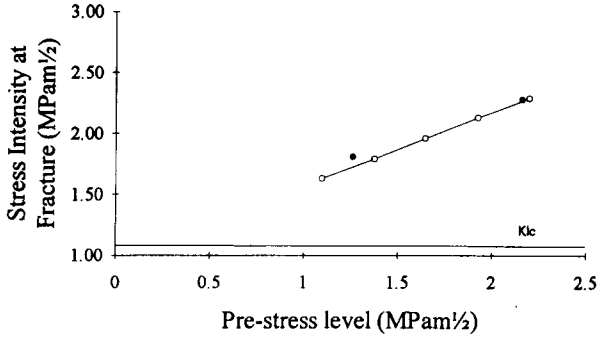

Fig. 5. The effect of pre-stressing level at 950°C on the room-temperature fracture toughness, compared with the fracture toughness predicted by the dislocation shielding model. ●, Measured toughness: ○, predicted toughness.

The fracture toughness was evaluated from the Vickers indentation radial crack lengths for indentation loads between 100 g and 1000 g. The toughness was calculated using the formula of Anstis *et al.*[18] and the previously determined hardness to Young's modulus ratio. The average fracture toughness was 1·020 ± 0·05 MPa$\sqrt{m}$. Comparable values were obtained using alternative formulae for indentation half-penny cracks.[19–21]

3 Modelling

The brittle/ductile transition was modelled by computer simulation of the evolution of a crack-tip dislocation array, using the method of Hirsch & Roberts.[22] The geometry of the model is shown in Fig. 6. The dislocation loops emitted from the crack tip are modelled as an array of infinite parallel straight dislocations moving on a slip plane perpendicular to the crack plane. The modelled dislocations are emitted from a source close to the crack tip when the stress on a notional dislocation at the source position is such as to move the dislocation away from the crack tip. The position of the source is adjusted so as to produce the first dislocation emission at the stress intensity value, K_N similar to that found by experiment (see, for example, Ref. 1). At each stage of the simulation, the stress on each dislocation is calculated, taking into account the applied stress intensity, interactions with all other dislocations, and the image forces due to the presence of the crack surface.[22] The velocity of each dislocation, v, is then calculated, according to the relation:

$$v = A\tau^m e^{-U/kT} \qquad (1)$$

where m is relatively insensitive to temperature and U is the activation energy for dislocation motion. A is a constant and k is the Boltzman constant. Each dislocation is moved a distance equal to its velocity multiplied by a small time

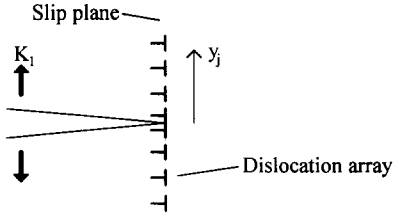

Fig. 6. The mode I two-dimensional approximation for edge dislocation emission and crack-tip shielding. The dislocations are located at positions y_j with an applied stress intensity factor K_I.

interval; the computer simulation repeats this process, giving the position of each dislocation in the array as a function of time in a simulated test.

The local stress intensity factor at the crack tip, K_{ez} due to dislocation shielding under a remote applied mode I stress intensity factor, K_I, is given by:

$$K_{ez} = K_t - \sum_{y_j \geq d_{crit}} \frac{3\mu b}{4(1-\nu)\sqrt{\pi y_j}} \qquad (2)$$

where μ is the shear modulus, ν, Poisson's ratio, b, the magnitude of the Burgers vector and y_j gives the individual positions in a dislocation array. The critical distance, d_{crit}, is the minimum distance dislocations must travel before shielding the most highly stressed section crack tip, and incorporates the three-dimensional geometry of the crack and dislocation sources.[1,5,7] Fracture is assumed to occur when K_{ez} exceeds the critical stress intensity factor for cleavage, K_{Ic}. At fracture, the applied stress intensity K_F may be greater than K_{Ic} because of the shielding action of the dislocations. The computer simulation of experimental fracture tests is used to determine the predicted variation of K_F with temperature (the modelled BDT curve). Further details of the model and justification of the fundamental simplifying assumptions are given in Refs 1, 5 and 22.

Parameters to be used in the model were found as follows. The Poisson's ratio and shear modulus were determined from a Voigt average[23] of high-temperature elastic constant measurements in Y_2O_3–ZrO_2, determined up to 1180°C[24,25] giving μ = 70 GPa, ν = 0·3. The length of the Burgers vector, b, is 7·28 Å.[24]

K_{Ic} was taken to be 1·1 MPa$\sqrt{m}$. The loading rate, dK/dt, was 1·2 × 10^{-4} MPa$\sqrt{m}$ s^{-1}, equivalent to the crosshead displacement rate of 1 μm min^{-1} for a typical crack size of 25 μm. K_N, the stress intensity for the first dislocation emission, was assumed to be 0·2 K_{Ic}. Previous studies (e.g. Ref. 2) have shown that a 'smooth' brittle/ductile transition, with fracture K rising steadily with test temperature, is characteristic of easy dislocation emission from crack-tip sources; modelling such

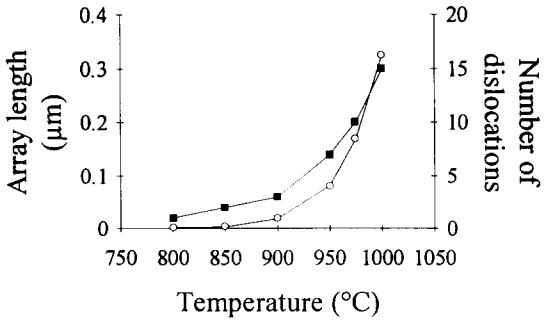

Fig. 7. The dislocation array length (○) and number of dislocations (■) emitted immediately before fracture, predicted by the dislocation shielding model.

behaviour[22] showed that,provided K_N is less than approximately 0·8 K_{Ic}, the behaviour of the model is not sensitive to the exact value of K_N. It was assumed that all emitted dislocations immediately contribute to crack shielding, and therefore d_{crit} was set to zero.

The model used the dislocation velocity data for {001} slip in 9·4 mol% Y_2O_3–ZrO_2 of Farber & Heuer[24] (determined above 1100°C). These data gave $m = 1{\cdot}4$, $U = 5$ eV and $A = 6{\cdot}7 \times 10^4$ for v in m s^{-1}, τ in MPa and T in degrees Kelvin.

The predicted fracture toughness as a function of temperature is compared with the experimental results in Fig. 2. The agreement with the observed fracture toughness is good, although the simulation underestimates the fracture toughness above 950°C. The dislocation array lengths and number of dislocations emitted prior to fracture are shown in Fig. 7. Very few dislocations are predicted to be active at the crack tip even at the highest test temperatures. Simulations of the warm pre-stressing experiments were also carried out using the same parameters. The results are shown in Fig. 5, and agree well with the observed warm pre-stressing effect.

4 Discussion

The Vickers and Knoop hardness and the H/E ratio were comparable with values in the literature for Y_2O_3–ZrO_2.[9,10,14] There was also good agreement with literature values for the room-temperature fracture toughness of cleavage on {110}, determined by Vickers indentation.[8,9] The similarity between the independently determined indentation toughness and the fracture toughness from pre-cracked specimens indicates that the pre-cracking procedure produces a well-defined crack, free from significant residual stresses. The average room-temperature fracture toughness value of 1·1 MPa$\sqrt{m}$ was therefore used in the model calculations.

The cubic zirconia showed a smooth brittle/ductile transition between 800°C and 1000°C, yielding at a surface stress of approximately 660 MPa at 1000°C. The toughness increase was not seen at high strain rates and the load/displacement trace showed no evidence of general yielding below 1000°C. Pre-stressing at 950°C to stress intensity factors above the room-temperature fracture toughness caused a toughness increase which was preserved on rapid cooling to room temperature. The absence of toughening at the higher loading rate at 1000°C (Fig. 2) shows that the toughness increase was not due to residual stress relief, but was due to dislocation shielding of the pre-crack.

The small size of the indentation plastic zone after high-temperature stressing, compared to the pre-crack size, implies that the dislocation sources nucleated at the indentation were not responsible for the crack shielding. The features observed on the fracture surface after etching (Fig. 4(b)) might result in selective etching at dislocations nucleated by general yielding. However, they resemble etch hillocks[26] and are more probably a surface contamination artefact and are unrelated to the internal structure. The tendency for etchant attack at the crack tip in the high temperature tests is indicative of crack-tip shielding by a high density of dislocation sources at, or close to, the crack tip, but with the emitted dislocation travelling only a small distance.

The dislocation shielding mechanism is supported by the agreement between the dynamic dislocation model and both the observed brittle/ductile transition (Fig. 2) and the warm pre-stressing effect (Fig. 5). The higher toughness value at 975°C may be due to an additional shielding contribution from yielding near the brittle/ductile transition temperature. The sub-micron dislocation array lengths predicted by the simulations (Fig. 7) would not be measurable by etching techniques.

The material-dependent parameters, μ, ν and b, used in the model, are relatively insensitive to composition,[24,25] and the expected error in their values does not have a significant effect on the simulation results. The model is sensitive to the choice of K_{Ic}, although this value is validated by the indentation and room-temperature fracture tests. The low value of K_N the stress intensity factor for dislocation source operation, is based on the operation of crack tip dislocation sources in silicon.[27] Its value does not significantly influence the simulation except when only one or two dislocations are emitted.

The critical distance, d_{crit}, has previously been used in silicon[1,5], sapphire[6] and germanium[7] to characterise the distance which dislocations must

travel from a few discrete sources on the crack front to shield the entire crack. Typically, d_{crit} is of the order of half the crack size for a semi-circular pre-crack. In silicon, the dislocation source operation was concentrated where the slip plane was tangential to the crack front.[1]

For the slip plane/crack geometry here, the resolved shear stress on the most favourably oriented glide plane in zirconia was calculated, using the solution for an embedded circular flaw as an approximation to a semi-circular flaw.[1,28] Glide on both the {100} and {111} slip systems were considered individually and simultaneously, although {100} slip is considered more probable and is indicated by the slip traces at 1000°C. It was found that for a crack parallel to (110), there were no positions around the crack front where dislocation source operation was particularly favoured by a significantly high maximum resolved shear stress on any individual slip system. Given easy dislocation source nucleation, demonstrated by the smooth transition (modelled using a low value of K_N) a high density of dislocation sources was therefore assumed to operate around the entire crack front; all emitted dislocations act to shield the crack tip and $d_{crit} = 0$.

In summary, the elastic constants and dislocation velocity behaviour are known to sufficient accuracy for their errors to have no significant effect on the simulation. The dislocation source nucleation and operation parameters may be justified by comparison with other brittle materials and the observed smooth brittle/ductile transition. The chosen value of d_{crit} is consistent with the cleavage plane and the available slip systems, assuming a high density of dislocation sources.

Some error between the observed and predicted brittle/ductile transition is to be expected due to the variation of mode I stress intensity around the crack front. The crack is not a perfect semi-ellipse and the stress intensity is not constant around the crack front. The etchant attack at the crack tip (Fig. 4(b)) and the fracture surface topography (Figs 3 and 4) both indicate that the stress intensity is at a maximum at the deepest point and shielding may not be uniform around the crack. However, despite the severe approximation of the two-dimensional mode I edge dislocation model and the use of an average stress intensity factor for the semi-elliptical crack, the good agreement suggests that the important features of the model are valid, although the near-exact coincidence of the experimental results and prediction (Fig. 2) may be fortuitous. The smooth brittle/ductile transition in cubic zirconia may therefore be understood by mobility-controlled dislocation shielding of the crack tip.

5 Conclusion

The room-temperature fracture toughness determined via the indentation technique and bend testing of pre-cracked specimens is approximately $1{\cdot}1 MPa\sqrt{m}$.

The brittle/ductile transition of cubic stabilised zirconia at a loading rate of $1{\cdot}2 \times 10^{-4}$ $MPa\sqrt{m}$ s^{-1} is characterised by a smooth increase in fracture toughness above 800°C; the specimens yielded at 1000°C. Pre-stressing at 975°C increased in the room temperature fracture toughness in a controllable manner.

The dynamic dislocation crack shielding model has been successfully applied to cubic zirconia. The important parameters in the model are determined by material constants and the test geometry. Good agreement was obtained between the model predictions and experimental observations. It is concluded that the brittle/ductile transition in cubic zirconia is controlled by the mobility of dislocations emitted at the crack tip.

Acknowledgements

The authors would like to thank Professor R. J. Brook for provision of laboratory facilities. The research was funded by SERC grant GR G 42853.

References

1. Hirsch, P. B., Roberts, S. G. & Samuels, J., The brittle–ductile transition in silicon. II. Interpretation. *Proc. R. Soc. London, A*, **421** (1989) 25–53.
2. Warren, P. D., The brittle/ductile transition in silicon: the influence of pre-existing dislocation arrangements. *Scripta Metall.*, **23** (1989) 637–42.
3. Booth, A. S., Cosgrave, M. & Roberts, S. G., The warm-prestressing effect in Silicon. *Acta Metall.*, **39** (1991), 191–7.
4. Ellis, M., The brittle to ductile transition in bcc metals. PhD Thesis, University of Oxford, (1991).
5. Hirsch, P. B. & Roberts, S. G., Modelling the brittle-ductile transition. In *Symposium on Materials Modelling: From Theory to Technology*, Oxford. IOP Publishing, (1991) pp. 181–6.
6. Roberts, S. G., Kim, H. S. & Hirsch, P. B., The brittle–ductile transition and dislocation mobility in silicon and sapphire. In *International Conference on the Strength of Metals and Alloys:* **9**, Haifa. (1991) pp. 317–24.
7. Serbena, F. & Roberts, S. G., The brittle–ductile transition in germanium. *Acta Metall.*, (1994), in press.
8. Stanescu, J. D. & Chan, M., Indentation study of fracture toughness anisotropy in cubic zirconia single crystals. *J. Mat. Sci.*, **11** (1992) 1364–6.
9. Pajares, A., Guiberteau, F., Dominguez-Rodruiguez, A. & Heuer, A. H., Microhardness and fracture toughness anisotropy in cubic zirconia single crystals. *J. Am. Ceram. Soc.*, (1988) C332–C333.
10. Morscher, G. N., Pirouz, P. & Heuer, A. H., Temperature dependence of hardness in yttria-stabilised zirconia single crystals. *J. Am. Ceram. Soc.*, **74** (1991) 491–500.

11. Ingel, R. P., Rice, R. W. & Lewis, D., Room-temperature strength and fracture of zirconia-yttria single crystals. *J. Am. Ceram. Soc.*, **65** (1982) C108–C109.
12. Dominguez-Rodruiguez, A., Lagerlof, K. P. D. & Heuer, A. H., Plastic deformation and solid solution hardening of yttria-stabilised zirconia. *J. Am. Ceram. Soc.*, **69** (1986) 281–4.
13. McCartney, M. L., Donlon, W. T. & Heuer, A. H., Plastic deformation in Calcia-stabilised zirconia. *J. Mater. Sci.*, **15** (1980)1063.
14. Hannick, R. H. J. & Swain, M. V., Induced plastic deformation of zirconia. *Deformation of Ceramic Materials II*, eds. R. F. Tressler & R. C. Bradt. Plenum Press, New York, 1984, pp. 695–708.
15. Ingel, R. P., Lewis, D., Bender, B. A. & Rice, R. W., Temperature dependence of strength and fracture toughness of zirconia single crystals. *J. Am. Ceram. Soc.*, **65** (1982) C150–C152.
16. Raju, I. S. & Newman, J. C., Stress intensity factors for a wide range of semi-elliptical surface cracks in finite thickness plates. *Eng. Frac. Mech.*, **11** (1979) 817–29.
17. Marshall, D. B., Noma, T. & Evans A. G., A simple method for determining elastic modulus to hardness ratios using Knoop indentation measurements. *J. Am. Ceram. Soc.*, **65**, (1982) C175–C176.
18. Anstis, G. R., Chantikul, P., Lawn, B. R. & Marshal, D. B. I. A critical evaluation of indentation techniques for measuring fracture toughness. *J. Am. Ceram. Soc.*, **64** (1981) 533–8.
19. Tanaka, K., Elastic/plastic indentation hardness and indentation fracture toughness: the inclusion core model. *J. Mater. Sci.* **22** (1987), 1501–8.
20. Evans, A. G. & Charles, E. A., Fracture toughness determinations by indentation. *J. Am. Ceram. Soc.*, **59** (1976) 371–2.
21. Lawn, B. R. & Fuller, E. R., Equilibrium penny-like cracks in indentation fracture. *J. Mater. Sci.*, **10** (1975) 2016–24.
22. Hirsch, P. B. & Roberts, S. G., The dynamics of edge dislocation generation along a plane orthogonal to a mode I crack. *Scripta Metall.*, **23** (1989) 925–30.
23. Kelly, A. & MacMillan, N. H., *Strong Solids*. Monographs on Physics and Chemistry of Materials. Clarendon Press, Oxford, (1986) pp. 399–400.
24. Farber, B. & Heuer, A. H., (1993), unpublished data.
24. S. Kandil, H. M., Greine, J. D. R. & Smith, J. F., Single crystal elastic constants of yttria-stabilised zirconia in the range 20°C to 700°C. *J. Am. Ceram. Soc.*, **67** (1984) 341–6.
25. Botha, P. J., Chiang, J. C. H., Comins, J. D. & Mjwara, P. M., Behaviour of elastic constants, refractive index and lattice parameter of cubic zirconia at high temperatures. *J. Appl. Phys.*, **73** (1993) 7268–74,
26. Tuck, B., The chemical polishing of semi-conductors. *J. Mater. Sci.*, **15** (1975) 321–9.
27. Samuels, J. & Roberts, S. G., The brittle-ductile transition in silicon. I. Experiments., *Proc. R. Soc. London*, **A421** (1989), 1–23.
28. Sneddon, I. N., The distribution of stress in the neighbourhood of a crack in an elastic solid. *Proc. R. Soc. London*, **A187** (1946) 229–60.